




A high FBR low SAR and AMC-backed compact wearable antenna array for WBAN applications

Jun Chu, Chengzhu Du  and Haifeng Shu

School of Electronics and Information Engineering, Shanghai University of Electric Power, Shanghai, People's Republic of China

Research Paper

Cite this article: Chu J, Du C, Shu H (2024) A high FBR low SAR and AMC-backed compact wearable antenna array for WBAN applications. *International Journal of Microwave and Wireless Technologies*, 1–11. <https://doi.org/10.1017/S1759078724001041>

Received: 13 March 2024
Revised: 14 September 2024
Accepted: 3 October 2024

Keywords:

antenna array; artificial magnetic conductor (AMC); high front-to-back ratio (FBR); low specific absorption rate (SAR); WBAN; wearable antenna

Corresponding author: Chengzhu Du;
Email: duchengzhu@163.com

Abstract

In this paper, a wearable antenna array based on a 9×3 artificial magnetic conductor (AMC) array is proposed with the characteristics of compact, low profile, low specific absorption rate (SAR), high front-to-back ratio (FBR) and high gain for wireless body area network (WBAN) bands. The proposed wearable antenna consists of a four-element array and an AMC array. The size of antenna array loaded AMC is $137.7 \times 45.9 \text{ mm}^2$. The dielectric substrate of the antenna and the AMC structure are made of 0.1 mm liquid crystal polymer material, which is flexible and low profiled. The antenna operates from 5.62 to 6 GHz after the AMC structure is loaded. The gain increases by 3.23 dB, reaching 12.03 dB at 5.8 GHz. And the FBR value is raised by 26.04 dB. The highest SAR value of the simulated antenna on the human model is 0.0496 W/kg, far less than the US federal or EU requirements. After constructing and testing the antenna, the outcomes of the tests agreed with the results of the simulation. The flexible antenna array with AMC structure has good prospect in WBAN applications.

Introduction

The emergence of 5G communication technology strongly promotes applications such as Internet of Everything [1], health monitoring [2], telemedicine [3], and wearable antennas have become a hot spot for research. With the continuous development of antenna industry, realizing miniaturization [4], low profile [5], and high gain [6] has been the direction of antenna innovation. To guarantee the safety when apply to the human body, having the characteristics of low human radiation and high front-to-back ratio (FBR) [7] is importance.

There are many studies on wearable antennas. Many researchers have proposed wearable antennas using Rogers 3003 [7, 8], Rogers 4003 [9], felt [10], textile [11], etc. as dielectric substrates in order to explore the properties of various materials. Meanwhile, in order to make wearable antennas more widely used and flexible in applications, antennas with multifrequency [12] and broadband [13] characteristics are also hot spots of research. The majority of them cover the wireless body area network (WBAN) band's 2.4 and 5.8 GHz.

In wearable antenna design [14–23], it is critical to ensure safety when applied to the human body, primarily in terms of a low specific absorption rate (SAR) value and a high FBR. In terms of reducing human body radiation, common solutions are loaded electromagnetic band gap (EBG) structures [14, 15], metamaterials (MTM) [11], or artificial magnetic conductor (AMC) structures [16–18, 22] on the back of the antenna to increase the antenna gain and FBR value while lowering the antenna's backward radiation. In reference [19], a dual-band dual-polarization antenna has the characteristics of high isolation and low SAR values with Substrate Integrated Waveguide (SIW) cavities.

Recently, many wearable antenna arrays are proposed, where researchers have used flexible materials such as polyethylene terephthalate [20], jeans [21], polydimethylsiloxane (PDMS) [22], and polytetrafluoroethylene (F4BM) [23] in the design of antenna array. In reference [20], the author proposed a flexible antenna array by CPW feed, making it easier to integrate into biomedical systems. The antenna is made up of four units with a peak gain of 10 dB. In reference [21], a wearable four-element antenna array with jeans substrate is designed, and its maximum gain can reach 13.09 dB. The antenna array proposed in reference [22] is loaded with a uniplanar compact EBG (UC-EBG) reflector, the maximum antenna gain is 13.6 dB, and the SAR is 0.59 W/kg at 6 GHz, but the overall size is large. In reference [23], a dual-polarized flexible antenna array is proposed, which are loaded with AMC structures. However, the final simulated antenna gain is only 7.9 dB. Under the current research, with the development of communication systems, wearable antennas with smaller gains and larger size cannot meet the needs of diversified applications. Therefore, it is a challenging work to design a compact flexible antenna array with the characteristics of high FBR, high gain and low SAR.

This paper presents a wearable antenna array for WBAN 5.8 GHz loaded AMC structure. The antenna operates in the 5.62–6.0 GHz band with a relative bandwidth of 6.5%. The final size of

the antenna is $137.7 \times 45.9 \text{ mm}^2$. The AMC structure and the antenna array are composed on 0.1 mm thick flexible liquid crystal polymer (LCP) substrate. The back-loaded AMC structure enables the antenna to reach a gain of 12.03 dB at 5.8 GHz and a FBR value of 27.48 dB. The SAR value is reduced from 0.7906 to 0.0496 W/kg. The results show that the antenna has good application prospects in the field of wearable antennas. The innovations in the paper are: the antenna array is low profile and flexibility; the overall size of the antenna is reduced by miniaturized design; an AMC structure is loaded underneath the antenna array, which can effectively enhance the gain and FBR, and reduce the SAR value of the antenna.

Antenna design

Antenna element design

Figure 1 shows the exact structure of the antenna element. A 0.1 mm thick LCP dielectric substrate with a loss tangent of 0.002 and a relative permittivity of 2.9 is used in the suggested antenna. The front is a 50Ω feeder, and the background has an engraved H-shaped slot. The H-shaped slot is added to improve the impedance bandwidth of the antenna. The overall size of the element is $18 \times 16.5 \text{ mm}^2$, and the simulation bandwidth covers 5.5–6.21 GHz. The optimized geometric parameters of the proposed antenna are as follows: $LL = 16.5 \text{ mm}$, $WW = 18 \text{ mm}$, $H = 0.1 \text{ mm}$, $Wc = 16 \text{ mm}$, $Lf = 16 \text{ mm}$, $Lk = 8.5 \text{ mm}$, $M1 = 6 \text{ mm}$, $M2 = 3 \text{ mm}$, $Wf = 0.26 \text{ mm}$, $Lc = 1 \text{ mm}$, $G = 0.1 \text{ mm}$.

The antenna element design process is given in Fig. 2. Antenna I is the first design step, the front is a 50Ω feed line, and the background has an engraved H-shaped slot, which can expand the bandwidth of the antenna. Antenna II is the second design step, the original H-slot is changed to a double H-slot for reducing the size of Antenna I, and the feed line is extended to both sides to form a T-shaped structure. Through miniaturization, the final antenna element's total size has been lowered by 45%.

The S-parameters for both two antennas are presented in Fig. 3. Antenna I covers 5.31–6.45 GHz, and Antenna II covers

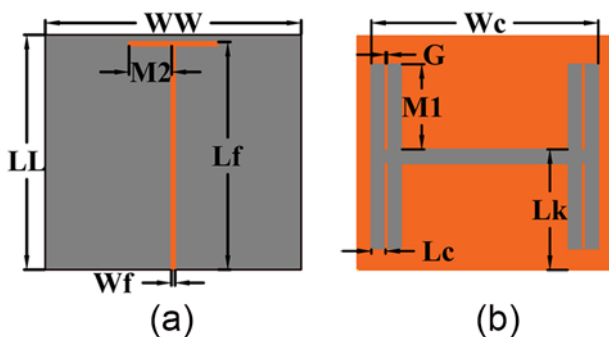


Figure 1. Antenna element structure diagram. (a) Top view (b) Back view.

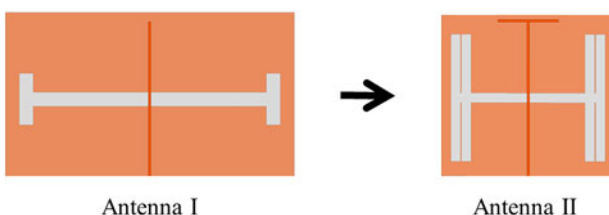


Figure 2. Design process of antenna element.

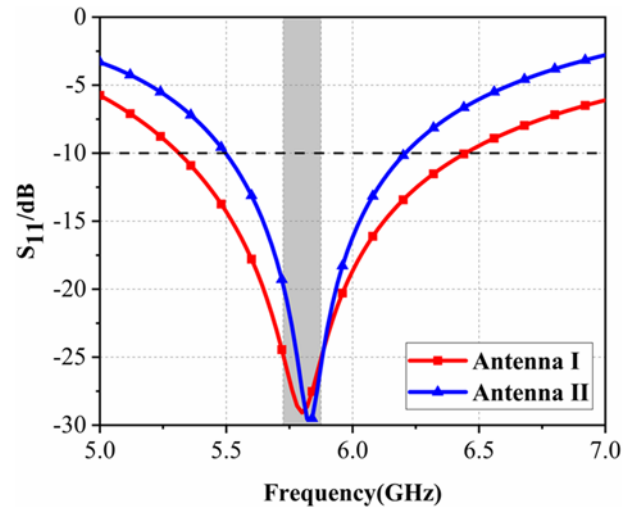


Figure 3. S_{11} of the two antennas.

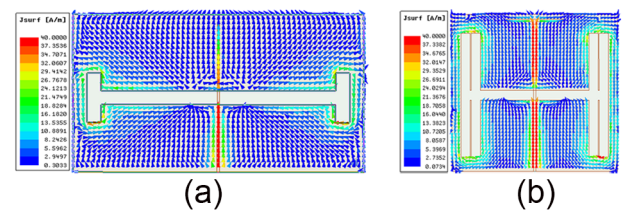


Figure 4. Current distribution diagrams. (a) Antenna I (b) Antenna II.

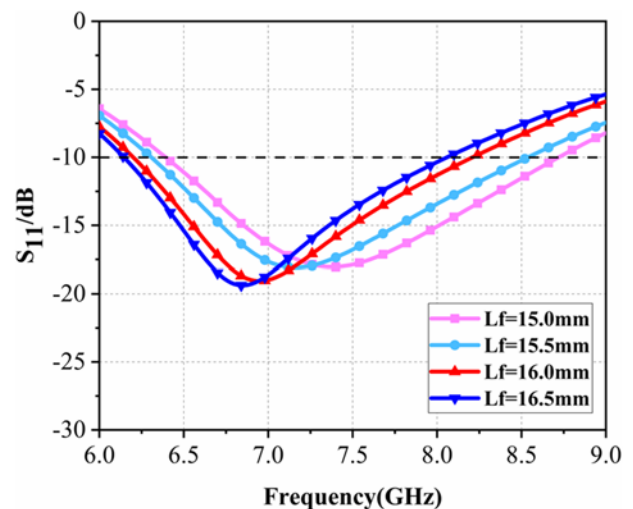


Figure 5. The influence of L_f on S_{11} .

5.5–6.21 GHz. After miniaturization, the bandwidth of the antenna is shortened by 0.43 GHz, but the reduced bandwidth of Antenna II still covers the desired frequency band. As the size of Antenna II is smaller, so it is chosen as the unit of the antenna array.

In Fig. 4 the current distribution of Antenna I and Antenna II at 5.8 GHz is given. From the figure we can notice that the current is mainly concentrated around the slit and feedline. The antenna's miniaturized design reduces the antenna's size while increasing the current path, which ensures that the antenna resonates at 5.8 GHz. Figure 5 gives the relationship between the length (L_f) and the antenna's resonance frequency. In the figure, when the L_f becomes

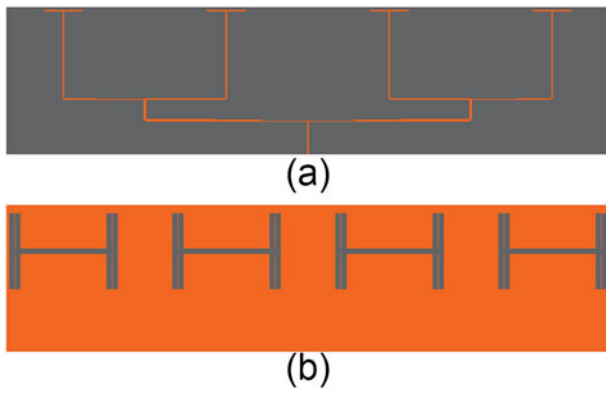


Figure 6. Antenna array structure. (a) Top view (b) Back view.

larger, the antenna’s electrical length increases, and the resonant frequency is more biased toward the low frequency.

Antenna array

Four antenna elements and the power divider are combined to form a quaternary antenna array, as shown in Fig. 6. The power divider is designed using the Chebyshev unequal division method to increase the antenna’s directivity. Overall antenna dimensions are 111 × 27 mm², and the spacing between adjacent units is 30 mm. Figure 7(a) displays the antenna array’s S₁₁ parameter, which covers 5.13–5.94 GHz. As the antenna resonance frequency will be shifted to the high frequency by adding AMC structure, so the antenna resonance frequency is set at 5.58 GHz. At 5.8 GHz, the realized gain and side lobe are 9.7 and –17.5 dB, respectively. The radiation pattern is shown in Fig. 7(b).

AMC unit

To lower the radiation toward the human body as well as to increase the FBR of the antenna, an AMC structure reflector is loaded on the back of the antenna array. When electromagnetic waves

are incident, the AMC structure has a high surface impedance, which can effectively reduce the backward radiation. It is also characterized by in-phase reflection, where the incident and reflected waves are superimposed to increase the forward gain.

In Fig. 8(a), the AMC reflection element is printed onto a 0.1 mm thick LCP dielectric substrate in the shape of a square patch. The metal ground plane completely covers the dielectric board’s rear surface. Figure 8(b) displays the AMC array’s corresponding circuit model. The AMC structure is equivalent to a LC parallel circuit. The gap between the patch and the ground will produce an equivalent capacitance C₁, and there is also an equivalent capacitance C₂ between two adjacent patches. The square patch on the upper layer generates an equivalent inductance L₁.

The proposed AMC structure is an evolution of the traditional mushroom-shaped structure. The size of AMC structure can refer to the following formula [24]:

$$L_1 = \mu_0 t \tag{1}$$

$$f_0 = \frac{1}{2\pi\sqrt{L_1 C_1}} \tag{2}$$

$$C_1 = \frac{\epsilon_0 (1 + \epsilon_r) w}{\pi} \cosh^{-1} \left(\frac{w + g}{g} \right) \tag{3}$$

where L₁ and C₁ stand for the AMC structure’s inductance and capacitance, ε₀ is the dielectric constant of free space, ε_r is the dielectric constant of the substrate, w is the width of the AMC square patch, g is the distance between the AMC patch, μ₀ is the permeability of the dielectric substrate, t is the dielectric substrate’s thickness, and f₀ is the operating frequency of the AMC structure. The optimized dimensions of the AMC element are as follows: w = 14.6 mm, g = 0.35 mm, t = 0.1 mm.

Figure 9 shows the design model and reflection phase characteristics of the AMC element, which has a reflection phase bandwidth of 60 MHz, covering 5.77–5.83 GHz. A model diagram of the proposed AMC array is given in Fig. 10. This AMC array consists of 9 × 3 units and the backside is completely covered by a metal ground.

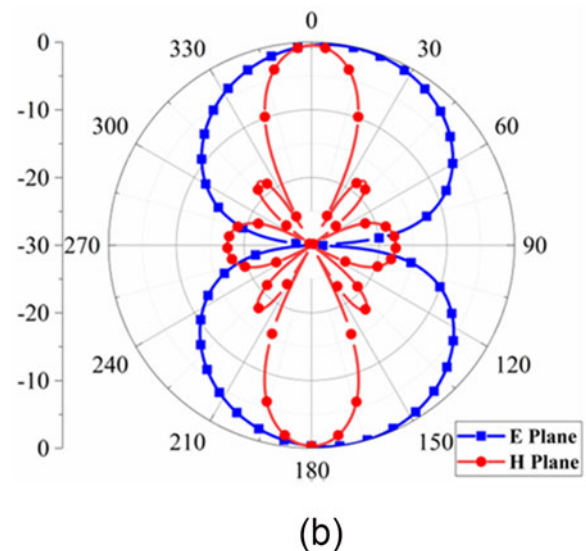
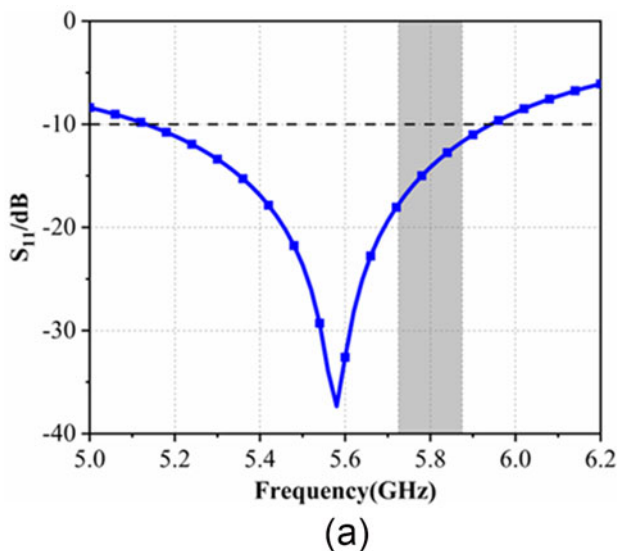


Figure 7. Antenna array performance. (a) S₁₁ parameter (b) Radiation pattern.

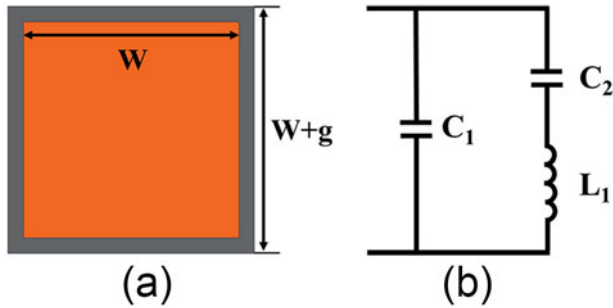


Figure 8. The proposed AMC unit. (a) AMC unit model (b) Equivalent circuit model.

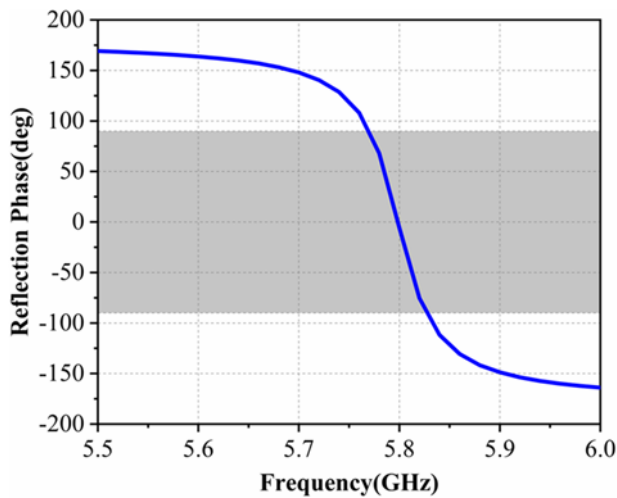


Figure 9. Reflection phase of the AMC unit.

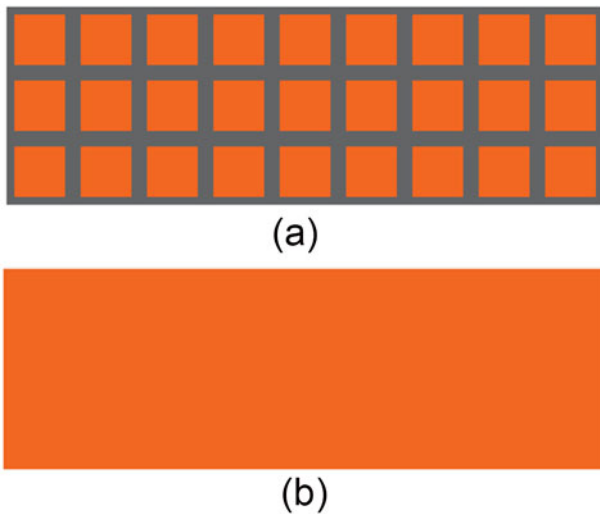


Figure 10. The structure of the AMC array. (a) Top view (b) Back view.

Antenna array loaded with AMC structure

The 9×3 AMC structure is loaded based on the antenna array, which is 11.8 mm away from the antenna array. During the simulation, the air-filled gap is between the array and AMC reflector. After loading the AMC reflector, the antenna's total dimensions are $137.7 \times 45.9 \text{ mm}^2$. The structure is shown in Fig. 11.

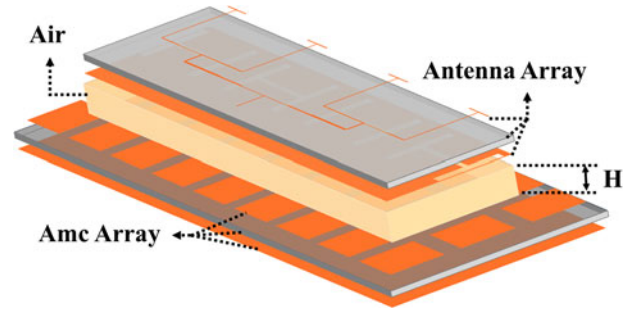


Figure 11. The AMC-loaded antenna array model.

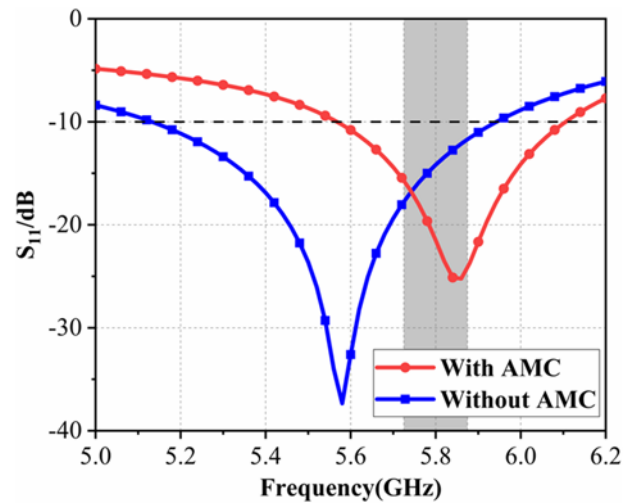


Figure 12. S_{11} parameters of the antenna.

The comparison of antenna S_{11} parameters before and after loading AMC is displayed in Fig. 12. Between 5.57 and 6.11 GHz, the AMC-loaded antenna's S_{11} is below -10 dB and covers the WBAN operating frequency band of 5.725–5.875 GHz. The relative bandwidth reaches 9.2%. Figure 13 shows the radiation pattern of the antenna before and after loading the AMC reflector at 5.8 GHz. From the figure, we can conclude that the antenna's backward radiation is significantly reduced after loading the AMC structure, and the forward gain increases. At 5.8 GHz, the antenna's gain is 13.5 dB., which is 3.8 dB higher than that without the AMC reflector structure. Furthermore, the FBR improves by 26.04 dB.

The surface currents at 5.8 GHz for the AMC unit and the array antenna loaded with the AMC structure are shown in Fig. 14. The maximum current density is observed at the floor gap section and at the front feeder. At the same scale, the surface current density of the 9×3 AMC structure placed behind the antenna array is significantly reduced and the back radiation is effectively reduced.

The effect of the distance H between the AMC and the antenna as well as the number of AMC units on the performance of the antenna is explored. Figure 15 gives the S_{11} parameters of the antenna after loading the AMC structure at varying values of H . As H increases, the resonant frequency point moves to the left. The FBR and realized gain values of the antenna at different H are given in Table 1. When H is taken as 11.8 mm, the S_{11} is from 5.58 to 6.1 GHz, the antenna realized gain is 13.5 dB, and the FBR is

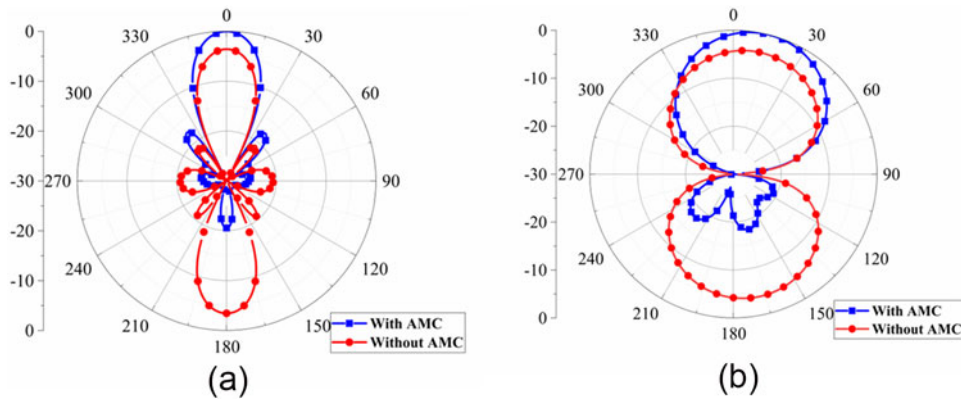


Figure 13. Radiation patterns with and without AMC structure at 5.8 GHz. (a) E plane (b) H plane.

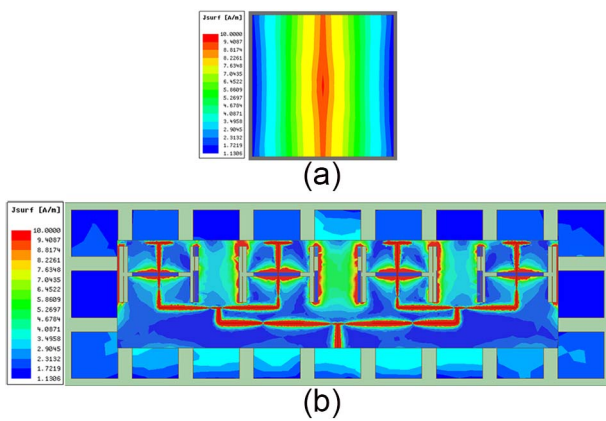


Figure 14. Surface current distribution. (a) AMC unit (b) Antenna array with AMC structure.

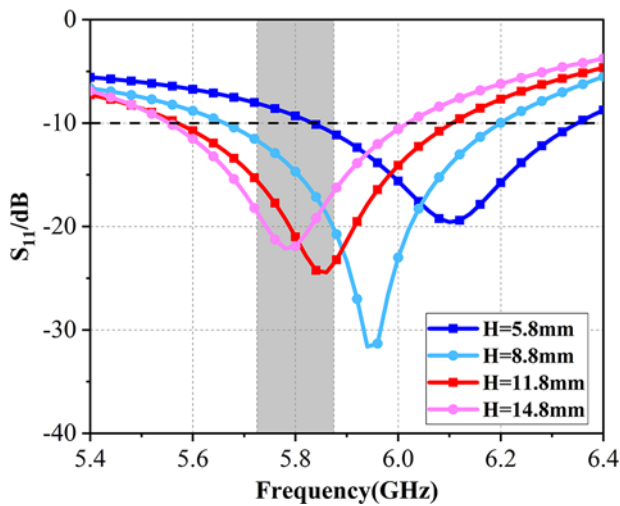


Figure 15. The effect of H on S_{11} parameters.

greatly improved to 27.48 dB, which can effectively reduce the radiation to the human body, so the optimum value of H is chosen as 11.8 mm.

To investigate the impact of varying ACM structures on the antenna, Fig. 16 provides the S_{11} parameters and radiation patterns of the antenna loaded with various AMC structures. As the

Table 1. The effect of H on FBR and realized gain values

H (mm)	FBR (dB)	Realized gain (dB)
5.8	22.11	13.4
8.8	23.93	13.7
11.8	27.48	13.5
14.8	28.62	13.0

number of AMC units increases, the impedance matching of the antenna gets better and the S_{11} value decreases gradually. The bandwidth and realized gain of the antenna with different sizes are given in Table 2. From the table it is clear that the bandwidth of the antenna is almost constant. With the enhancement of the AMC reflector plate size, the gain is improved. From Fig. 16(b) and (c), the EH-plane radiation patterns of the antenna are almost constant. Considering both size and performance, the AMC array size is finally selected 9×3 .

Figure 17 shows the S_{11} values of the antenna loaded by the AMC and Perfect Electric Conductor (PEC) structure, and the PEC reflector is the same size as the AMC structure. From the figure, it can be seen when the distance between the antenna and the PEC structure is gradually increased, the resonant frequency point moves to the left. When the distance H is 11.8 mm, the S_{11} of the antenna loaded with AMC structure is better than PEC structure. The FBR values of the antenna for different values of H are given in Table 3. When the H is 11.8 mm, the antenna loaded AMC structure is able to achieve higher FBR values than PEC structure. When the antenna is loaded by the PEC structure, the FBR value increases with the enhancement of H, but the space size is larger. In summary, the antenna loaded AMC structure can achieve a higher FBR value with a small size.

Measured results and analysis

S_{11} parameter

The proposed antenna was fabricated, as shown in Fig. 18. In a microwave anechoic chamber, the return loss and far-field radiation patterns of the antenna were measured.

The return loss of both the standalone antenna array and the antenna array loaded with an AMC structure was tested using a vector network analyzer. Figure 19 shows the measurement results. The measured S_{11} of the antenna array without AMC

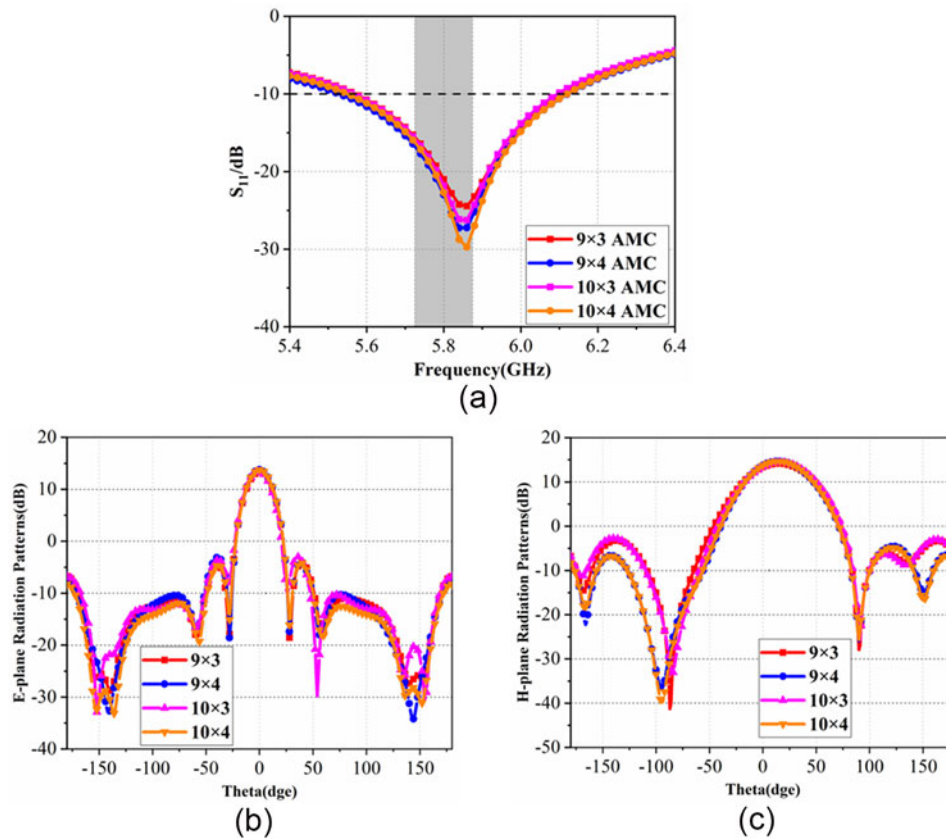


Figure 16. Effect of loading different number of AMCs on antenna performance. (a) Effects on S_{11} parameters (b) Effects on E-plane radiation (c) Effects on H-plane radiation.

Table 2. The performance of antennas with different numbers of AMC units

AMC array size	Bandwidth (GHz)	Realized gain (dB)
9 × 3	5.57–6.11	13.5
9 × 4	5.52–6.12	13.8
10 × 3	5.57–6.09	13.54
10 × 4	5.55–6.12	13.89

Table 3. The FBR values for different values of H

H (mm)	FBR (dB)
11.8(With PEC)	25.6
13.8(With PEC)	28.1
15.8(With PEC)	27.7
17.8(With PEC)	26.3
11.8(With AMC)	27.48

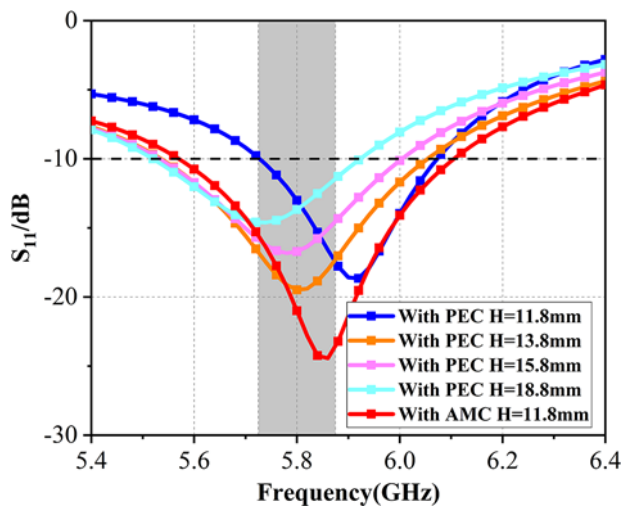


Figure 17. Simulated S_{11} of the antenna supported by the AMC and PEC structure.

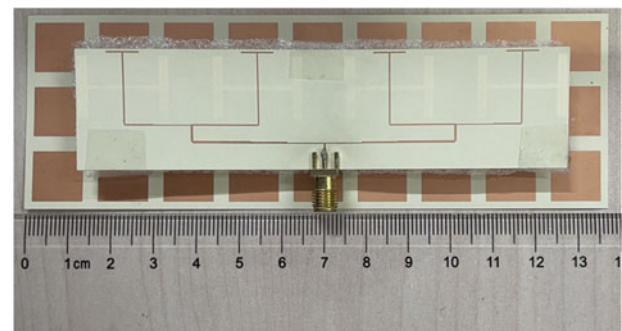


Figure 18. Antenna physical diagram.

structure covers 5.22–5.88 GHz. After loading the AMC structure, the S_{11} covers 5.62–6 GHz, achieving a relative bandwidth of 6.5%. Compared with the simulation data, the measured return loss and

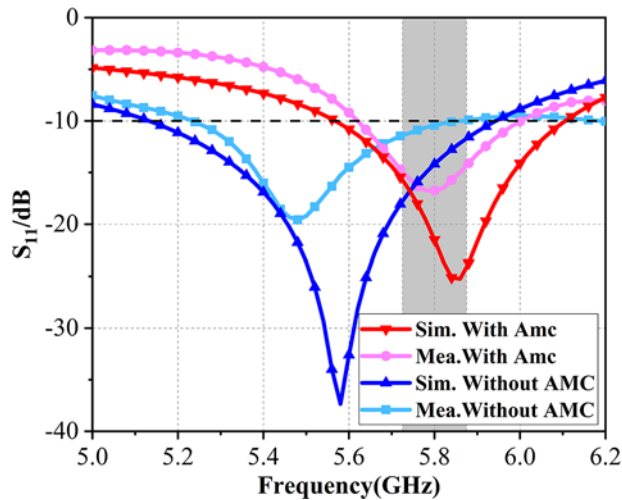


Figure 19. Comparison of measured and simulated data.

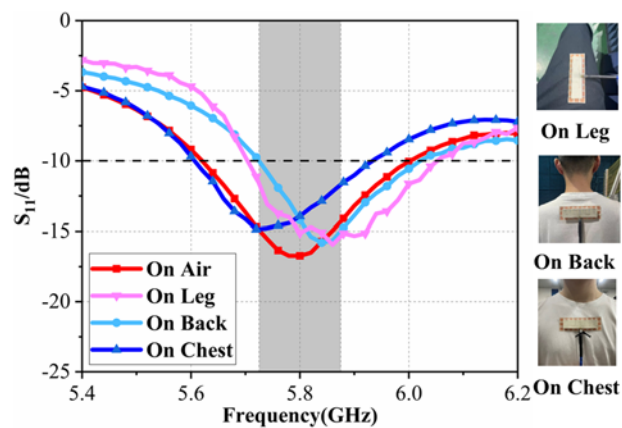


Figure 20. Measured S_{11} parameters on different body parts.

bandwidth exhibit some deviations, as well as the measured resonant frequency shifts to 5.8 GHz. These differences in measurement results may be due to machining errors and the test environment.

The antenna was placed on the back, chest, and legs of the human body, to test its performance. The measured S_{11} is shown in Fig. 20, which is less than -10 dB in the required frequency band of 5.725–5.875 GHz, indicating good performance.

Far-field radiation

The radiation pattern and gain of the antenna are tested in the far-field darkroom. Figure 21 displays the antennas' 5.8 GHz simulated and measured radiation patterns. From the figure we can see that the test results are basically consistent with the simulation results. The antenna's backward radiation is effectively reduced. After loading AMC, the simulated side lobe of the antenna is -17.6 dB, and the measured side lobe can only reach -13.1 dB due to the influence of test error.

In Fig. 22(a), the measured and simulated gain comparison of the antenna with and without AMC structure is given. After loading the AMC array, the gain is increased from 8.8 dB to 12.03 dB at 5.8 GHz, which is increased by 3.23 dB. The measured gain is reduced by about 1.5 dB compared with the simulation results. The variance in measurement and environmental uncertainty is the reason for the deviation of the results. In Fig. 22(b), the FBR value of the antenna array without AMC structure at 5.8 GHz is 1.44 dB. After loading AMC, the FBR becomes 27.48 dB at 5.8 GHz. In Fig. 23, the radiation efficiency plot of the antenna loaded with AMC structure is given. In the simulation results, the radiation efficiency is over 90%. The measured radiation efficiency of the antenna is higher than 80% within the desired frequency band 5.725–5.875 GHz, which provides good radiation results. The discrepancy between the over 90% simulated radiation efficiency and the smaller 80% measured radiation efficiency due to factors such as machining errors in processing the antenna, testing errors, and the environment surrounding the antenna during testing.

SAR evaluation

As wearable device, the SAR of the antenna needs to be evaluated. The SAR value is a parameter to measure the amount of electromagnetic radiation energy absorbed by a substance. The US federal standards require that SAR values are less than 1.6 W/kg, while the European federal standard is not more than 2 W/kg.

Figure 24(a) shows a simulation model of SAR values based on 10 g of human tissue. A four-layer human tissue model is constructed in HFSS, which is skin, fat, muscle, and bone from the surface to the inside. The distance between the antenna array and human model is 3 mm in the simulation. Figure 24(b) shows the simulated S_{11} of the antenna with and without the human body. Since the human model is also a medium when placed on a human body model for simulation, the S_{11} becomes worse, but

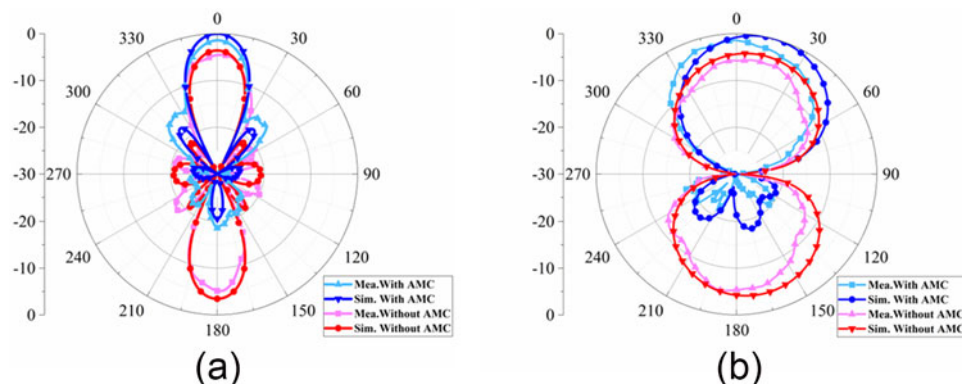


Figure 21. Far-field radiation patterns at 5.8 GHz. (a) E plane (b) H plane.

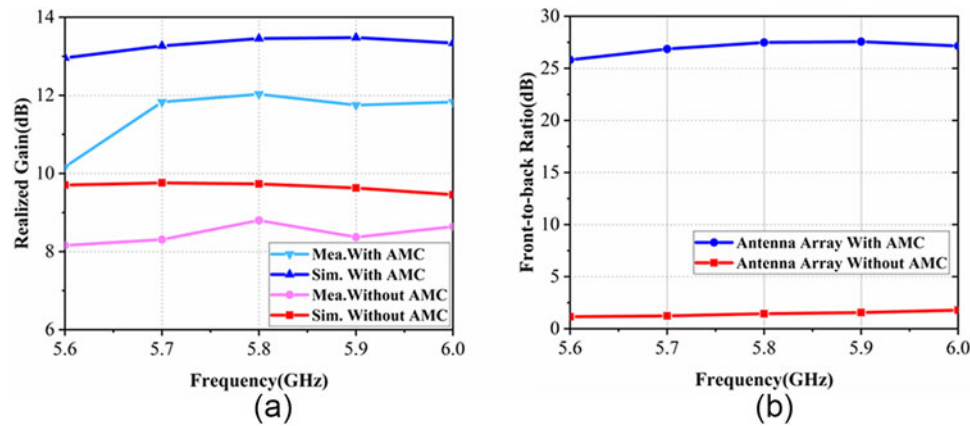


Figure 22. Comparison of antenna array performance with and without AMC. (a) Realized gain (b) FBR value.

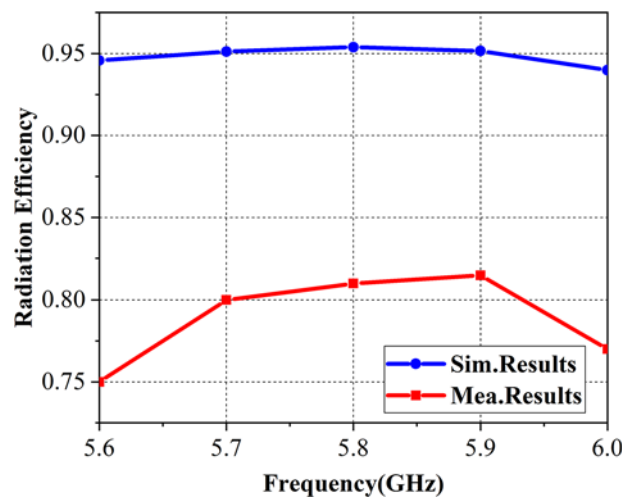


Figure 23. Radiation efficiency of antenna loaded AMC structure.

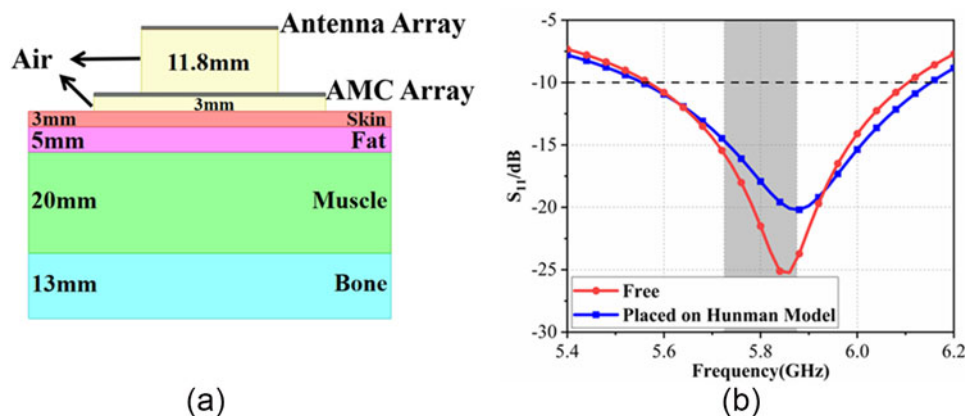


Figure 24. SAR value simulation. (a) Simulation model (b) S_{11} parameters.

the operating frequency band is almost unaffected and can cover 5.55–6.15 GHz. The electromagnetic properties of the layers of the mannequin are shown in Table 4.

Figure 25 shows the simulation results of the SAR value at 5.8 GHz. The SAR values with and without AMC structure are compared in the figure. According to the results, SAR field of

antenna array on the human body with AMC structure is significantly reduced.

Table 5 shows the effect of the size of the AMC array on SAR values. From the table it can be seen that the larger the size of the AMC array, the lower the SAR value. The SAR values with varying H are discussed in Table 6. It can be seen that the larger the distance

Table 4. Electromagnetic properties of various human tissues

	Bone	Muscle	Fat	Skin
ϵ_r	18.49	52.67	5.27	37.95
σ (S/m)	0.82	1.77	0.11	1.49
Density(kg/m ³)	1008	1006	900	1001
Thickness(mm)	13	20	5	3

H from the antenna to the human body, the smaller the SAR value.

Performance comparison

The performance comparison between the proposed wearable antenna array loaded with AMC and the previously proposed antennas is given in Table 7. In references [8–10, 19], a single antenna loaded reflector design is used such as AMC, MTM, and SIW, and the gains of the antennas are less than 8.2 dB. In reference [21], wearable antenna without AMC structure have narrow bandwidth, and the FBR values aren't presented. In reference [22], the antenna is loaded with UC-EBG structure to achieve wide bandwidth and high gain. However, its size is large and its SAR is 0.59 W/kg at 6 GHz. In reference [23], the final simulated gain

Table 5. The effect of AMC array size on SAR values

AMC array size	H (mm)	SAR (W/kg)
9 × 3	3	0.0495
9 × 4		0.0423
10 × 3		0.0472
10 × 4		0.0207

Table 6. The effect of H on SAR values

AMC array size	H (mm)	SAR (W/kg)
9 × 3	1	0.0536
	2	0.0515
	3	0.0495
	4	0.0439
	5	0.0346

of a dual-polarized antenna array with AMC structures is only 7.9 dB. In summary, the wearable antenna array with loaded AMC structure proposed in this paper is characterized by low SAR, high FBR, high gain, and compact size.

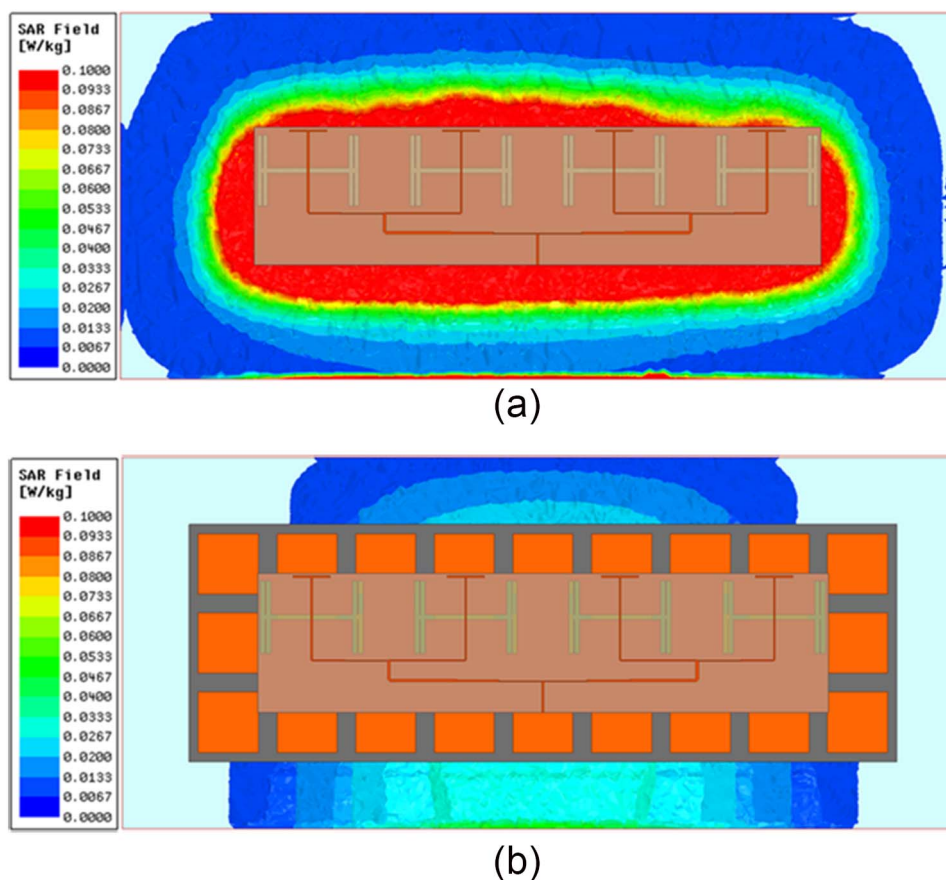
**Figure 25.** The changes of SAR value without and with loading AMC. (a) SAR value without AMC (b) SAR value with AMC.

Table 7. Comparison of antenna performance

Ref.	Size (mm ²)	Material	Flexibility	Bandwidth (GHz)	Gain (dB)	SAR (W/kg)	FBR enhancement (dB)	Element	Type
[8]	90 × 90	Rogers 3003	Semiflexible	2.2–2.85(25.7%) 5.68–6.29(10.1%)	4.8 7.7	0.28 0.752	12 20	1	Single + AMC
[9]	43.2 × 43.2	Rogers 4003	Semiflexible	5.725–5.85(2.1%)	8.2	0.562	19	1	Single + AMC
[10]	85 × 85	Felt	Flexible	6–12(66.7%)	9.08	1.046	15	1	Single + MTM
[19]	51.9 × 51.9	Rogers 5880	Semiflexible	5.1–5.35(4.7%) 5.68–5.85 (2.9%)	6.2 6.9	0.205 0.31	–	1	Single + SIW
[21]	140 × 60	Jeans	Flexible	5.34–5.46(2.2%)	13.09	–	–	4	Array
[22]	170 × 70	PI, PDMS	Flexible	4.5–6.5(36.3%)	13.6	0.59	–	4	Array + UC-EBG
[23]	144 × 48	F4BM 220	Flexible	5.25–6.06(14.3%)	7.9	0.54	–	4	Array + AMC
Prop.	137.7 × 45.9	LCP	Flexible	5.62–6(6.5%)	12.03	0.0496	26.04	4	Array + AMC

Conclusion

This paper presents a compact, low SAR, high gain, high FBR wearable flexible antenna array. The antenna operates at 5.8 GHz and covers 5.62–6 GHz. The antenna array gain is 12.03 dB at 5.8 GHz after loading the AMC structure, an improvement of 3.23 dB. At the same time, the FBR can reach 27.48 dB. The antenna's SAR value is only 0.0495 W/kg, which is far below the standard value. The compact flexible antenna array with low SAR, high FBR, and high gain is suitable to human health monitoring, human wireless communication, and telemedicine applications in the WBAN band.

Competing interests. The authors report no conflict of interest.

References

- Dixit AS and Kumar S (2023) Antipodal Vivaldi antenna with enhanced gain and improved radiation patterns for 5G-IoT applications using metamaterial and substrate integrated waveguide. *AEU-International Journal of Electronics and Communications* **161**, 154549.
- Zhao Z, Zhang C, Lu Z, Chu H, Chen S, Liu M and Li G (2023) A miniaturized wearable antenna with five band-notched characteristics for medical applications. *IEEE Antennas and Wireless Propagation Letters* **22**, 1246–1250.
- Alqadami ASM, Nguyen-Trong N, Mohammed B, Stancombe AE, Heitzmann MT and Abbosh A (2019) Compact unidirectional conformal antenna based on flexible high-permittivity custom-made substrate for wearable wideband electromagnetic head imaging system. *IEEE Transactions on Antennas and Propagation* **68**(1), 183–194.
- Wang G, Xuan X, Jiang D, Li K and Wang W (2022) A miniaturized implantable antenna sensor for wireless capsule endoscopy system. *AEU-International Journal of Electronics and Communications* **143**, 154022.
- Nikam PB, Kumar J, Baidya A and Ghosh A (2022) Low-profile bandwidth and E-plane radiation pattern reconfigurable patch antenna for sub-6 GHz 5G applications. *AEU-International Journal of Electronics and Communications* **157**, 154415.
- Ibrahim AA and Ali WAE (2021) High gain, wideband and low mutual coupling AMC-based millimeter wave MIMO antenna for 5G NR networks. *AEU-International Journal of Electronics and Communications* **142**, 153990.
- Pei LR, Du C, Shi CX and Peng H (2022) A gain enhanced low SAR dual-band MIMO antenna integrated with AMC for wearable ISM applications. In *2022 7th International Conference on Communication, Image and Signal Processing (CCISP)*. IEEE, 371–375.
- Yadav M, Ali M and Yadav RP (2021) Gain enhanced dual band antenna backed by dual band AMC surface for wireless body area network applications. In *2021 IEEE Indian Conference on Antennas and Propagation (InCAP)*. IEEE, 494–497.
- Mu G and Ren P (2020) A compact dual-band metasurface-based antenna for wearable medical body-area network devices. *Journal of Electrical and Computer Engineering* **2020**, 1–10.
- Muhammad HA, Abdulkarim YI, Abdoul PA and Dong J (2023) Textile and metasurface integrated wide-band wearable antenna for wireless body area network applications. *AEU-International Journal of Electronics and Communications* **169**, 154759.
- Das GK, Basu S, Mandal B, Mitra D, Augustine R and Mitra M (2020) Gain-enhancement technique for wearable patch antenna using grounded metamaterial. *IET Microwaves, Antennas & Propagation* **14**(15), 2045–2052.
- Dang QH, Chen SJ, Zhu B and Fumeaux C (2021) Dual-band dual-mode wearable textile antennas for on-body and off-body communications. In *2021 IEEE Asia-Pacific Microwave Conference (APMC)*. IEEE, 64–66.
- Varkiani SMH and Afsahi M (2019) Compact and ultra-wideband CPW-fed square slot antenna for wearable applications. *AEU-International Journal of Electronics and Communications* **106**, 108–115.
- Kumkhet B, Rakluea P, Wongsin N, Sangmahamad P, Thaiwirot W, Mahatthanajatuphat C and Chudpooiti N (2023) SAR reduction using dual band EBG method based on MIMO wearable antenna for WBAN applications. *AEU-International Journal of Electronics and Communications* **160**, 154525.
- Nie H, Xuan X and Ren G (2021) Wearable antenna pressure sensor with electromagnetic bandgap for elderly fall monitoring. *AEU-International Journal of Electronics and Communications* **138**, 153861.
- Yang S, Yu C, Yang X and Zhao J (2023) A tri-band flexible antenna based on tri-band AMC reflector for gain enhancement and SAR reduction. *AEU-International Journal of Electronics and Communications* **168**, 154715.
- Youssef OM, Atrash ME and Abdalla MA (2023) A compact fully fabric I-shaped antenna supported with textile-based AMC for low SAR 2.45 GHz wearable applications. *Microwave and Optical Technology Letters* **65**, 2021–2030.
- Saha P, Mitra D and Parui SK (2021) Control of gain and SAR for wearable antenna using AMC structure. *Radioengineering* **30**(1), 81–88.

19. **Chaturvedi D, Kumar A and Althuwayb AA** (2023) A dual-band dual-polarized SIW cavity-backed antenna-duplexer for off-body communication[J]. *Alexandria Engineering Journal* **64**, 419–426.
20. **Farooq U, Iftikhar A, Fida A, Khan MS, Shafique MF, Asif SM and Shubair RM** (2019) Design of a 1×4 CPW microstrip antenna array on PET substrate for biomedical applications. In *2019 IEEE International Symposium on Antennas and Propagation and USNC-URSI Radio Science Meeting*. IEEE, 1345–1346.
21. **Reddy BRS, Vakula D and Kumar AA** (2018) Performance analysis of wearable antenna array for WLAN applications. In *2018 IEEE Indian Conference on Antennas and Propagation (InCAP)*, IEEE, 1–4.
22. **Zu H, Wu B, Yang P, Li W and Liu J** (2021) Wideband and high-gain wearable antenna array with specific absorption rate suppression. *Electronics* **10**(17), 2056.
23. **Huang R and Liu X** (2020) A wearable low-profile flexible dual-polarized antenna array loaded with AMC for 5 GHz WLAN on-/off-body applications. In *2022 IEEE MTT-S International Microwave Workshop Series on Advanced Materials and Processes for RF and THz Applications (IMWS-AMP)*, IEEE, 1–3.
24. **Ashyap AYI, Dahlan SHB, Abidin ZZ, Abbasi MI, Kamarudin MR, Majid HA, Dahri MH, Jamaluddin MH and Alomainy A** (2020) An overview of electromagnetic band-gap integrated wearable antennas. *IEEE Access* **8**, 7641–7658.



Jun Chu was born in Jiangsu, China in 1999. She received the B.S. degree from the Shanghai University of Electric Power in 2021. She is currently pursuing the M.S degree in College of Electronics and Information Engineering, Shanghai University of Electric Power. Her research interests include antenna array and multiband antenna.



and MIMO technologies.

Chengzhu Du was born in Haikou, Hainan Province, China. She received the B.S. degree from the Xidian University, M.S. degree from Nanjing University of Posts and Telecommunications and PhD degree from Shanghai University, in 1995, 2003, and 2012, respectively, all in electromagnetic wave and microwave technology. She is currently an associate Professor of Shanghai University of Electric Power. Her research interests include flexible antenna, multiband and wideband antennas,



Haifeng Shu was born in Sichuan, China in 1998. He received the B.S. degree from the Shanghai University of Electric Power in 2021. He is currently pursuing the M.S degree in College of Electronics and Information Engineering, Shanghai University of Electric Power. His research interests include antenna array and wearable antenna.